



Research Article

Microstructure and Mechanical Properties of Ultrafine Structured Al-4wt%Cu-(2.5-10) vol.%SiC Nanocomposites Produced by Powder Consolidation Using Powder Compact Extrusion

Amro A.Gazawi¹, Brian Gabbitas², Deliang Zhang³, Charlie Kong⁴, Paul Munroe⁵

^{1,2}Waikato Centre of Advanced Materials (WaiCAM), School of Engineering, The University of Waikato, Hamilton, New Zealand

³Shanghai Jiao Tong University, School of Materials Science and Engineering, 800 Dongchuan Road, 200240, Shanghai, China

^{4,5}Electron Microscopy Unit, The University of New South Wales, Sydney, Australia

Correspondence should be addressed to: Amro A. Gazawi; ag73@students.waikato.ac.nz

Received date: 15 April 2014; Accepted date: 29 May 2014; Published date: 4 December 2015

Academic Editor: Sri Bandyopadhyay

Copyright © 2015. Amro A.Gazawi, Brian Gabbitas, Deliang Zhang, Charlie Kong, Paul Munroe. Distributed under Creative Commons CC-BY 4.0

Abstract

Ultrafine structured Al-4wt. %Cu- (2.5-10) vol. % SiC nanocomposites were produced by high energy mechanical milling of a mixture of Al and Cu powders and SiC nano-powder to produce nanocomposites powders, followed by consolidation of the powders using powder compact extrusion (PCE). Scanning and transmission electron microscopy as well as tensile testing were used to characterize the extruded nanocomposite bars. Increasing the volume fraction of SiC nanoparticles from 2.5 to 5.0 causes the yield strength, ultimate tensile strength and microhardness of the nanocomposite to increase from 98 MPa, 168 MPa and 104 HV to 391 MPa, 400 MPa and 153 HV, showing the effectiveness of SiC nanoparticles and microstructural refinement in strengthening the material. However, the ductility decreases from 6.8% to 2%, possibly due to the existence of SiC nanoparticle agglomerates in the Al-4wt%Cu-5vol.%SiC nanocomposite. The ultrafine structured Al-4wt%Cu-(7.5 and 10)vol.%SiC nanocomposite bars fractured prematurely during tensile testing. The possible reason for this may be the existence of SiC nanoparticles agglomerates in their microstructure.

Keywords: Aluminium alloy matrix nanocomposite, powder metallurgy, mechanical properties, microstructure.

Introduction

Al alloy matrix composites (AMCs) synthesized using powder metallurgy have

been studied widely over several decades, due to the potential of such materials to have excellent mechanical properties such as high wear resistance, high strength and

improved modulus, as well as low density, which are all highly desirable for aerospace and automotive applications¹⁻¹³. By reducing the sizes of ceramic particles in AMC's to nanometer range (<100nm), there is a potential for offering higher strength and fracture toughness. In the fabrication of AMNCs, one of the challenges is the difficulty of dispersing nanometre sized ceramic particles homogeneously in the aluminium alloy matrix. One way of overcoming this difficulty is to produce AMNC powders with ceramic nanoparticles homogeneously dispersed in the Al or Al alloy matrix of each of the powder particles by high energy mechanical milling (HEMM) of mixtures of metallic powders and the ceramic nanopowders^{3,6,8,14}. The nanocomposite powders can be subsequently consolidated using severe plastic deformation processes such as powder compact forging and powder compact extrusion to produce near net shaped components or structural members^{2,7-9}. This approach has been used by Hesabi et al.¹¹ who synthesised nanostructured Al-5vol.%Al₂O₃ nanocomposite powder by HEMM, and consolidated the milled nanocomposite powder into bars by powder compact extrusion. Their study showed that the ultrafine grained structure of the Al matrix coupled with the Al₂O₃ nanoparticles produced the nanocomposite bars with a strength of 356 MPa and good ductility.

On the other hand, Ogel et al.¹³ used simple mixing of Al, Cu, and SiC powders and hot pressing to produce Al-5wt%Cu-(15,30) vol.%SiC metal matrix composites reinforced with micrometer sized SiC particles. They found that the strength of the material was improved with increasing amounts of SiC particles, but the ductility of the material was clearly reduced. The microstructural examination also revealed that the SiC particles were not homogeneously distributed in the Al alloy matrix, showing the difficulty with homogeneously dispersing SiC particles even in the fabrication of AMCs using powder metallurgy.

In this study, we utilised the approach of synthesizing nanostructured Al-4wt.%Cu-(2.5-10)%SiC nanocomposite powders

using HEMM, followed by consolidation of the milled nanocomposite powders by cold pressing and hot powder compact extrusion to obtain bulk ultrafine structured nanocomposite samples with a uniform distribution of SiC nano particles. The aim of the study is to elucidate the effect of the volume fraction of the SiC nanoparticles on the microstructure and mechanical properties of bulk ultrafine structured Al-4wt. %Cu-(2.5-10)%SiC nanocomposites.

Experimental Procedure

Preparation of the Powder

In this study, the aluminium powder was reinforced with 2.5, 5, 7.5, and 10 vol.% of SiC nanoparticles. The powders used were; Al (99.7% pure; mean particle size: 40µm), and Cu (99.7% pure; particle sizes <63µm) powders, SiC nanopowder (99.5% pure, particle sizes <100nm), and 1wt% of stearic acid which worked as a process control agent (PCA).

Preparation of the nanocomposites

To produce the nanocomposite powders, the powders were first mixed under argon for 6 hours with a Restch PM100 planetary ball mill and a rotational speed of 100 rpm. Then, the powder mixture was milled for a net time of 12 hours with a rotational speed of 400rpm using the same ball mill.

The nanocomposite powders produced were compacted by using uniaxial pressing at room temperature for 5 minutes under a pressure of 1000 MPa with a cylindrical H13 steel die (internal diameter: 25mm). The powder compacts were heated to 500 °C using induction heating under argon, and then extruded to produce cylindrical bars with diameter of 8 mm. The extrusion cylinder speed was 7.7mm/s.

Characterization

The density of the extruded bars was measured using Archimedes method. Flat dog-bone shaped tensile test specimens with a gauge length of 20 mm were cut from the extruded bars using an electrical discharge machine (EDM) wire cutter, and

tested at room temperature using an Instron 4204 testing machine with a strain rate of $1.8 \times 10^{-4} \text{ s}^{-1}$. Scanning electron microscopy (SEM), transmission electron microscopy (TEM) and X-ray diffractometry (XRD) were used to characterize the microstructure of the extruded bars and fractured tensile test specimens. The microhardness of the extruded bars was measured using a Vickers microhardness tester with a load of 25-g and a loading duration of 15-s.

Results and Discussion

The microhardness of samples produced by powder compact extrusion (PCE) was measured and an average was taken of 15 indents. The average microhardness of the Al-4wt.%Cu-(2.5-10) vol. %SiC nanocomposite bars produced by PCE increased from 104 HV to 205 HV with increasing volume fraction of SiC nanoparticles from 2.5 to 10%. This can be compared with the microhardness of the milled nanocomposite powders, which increased from 122 HV to 192 HV, as shown in Fig.1.

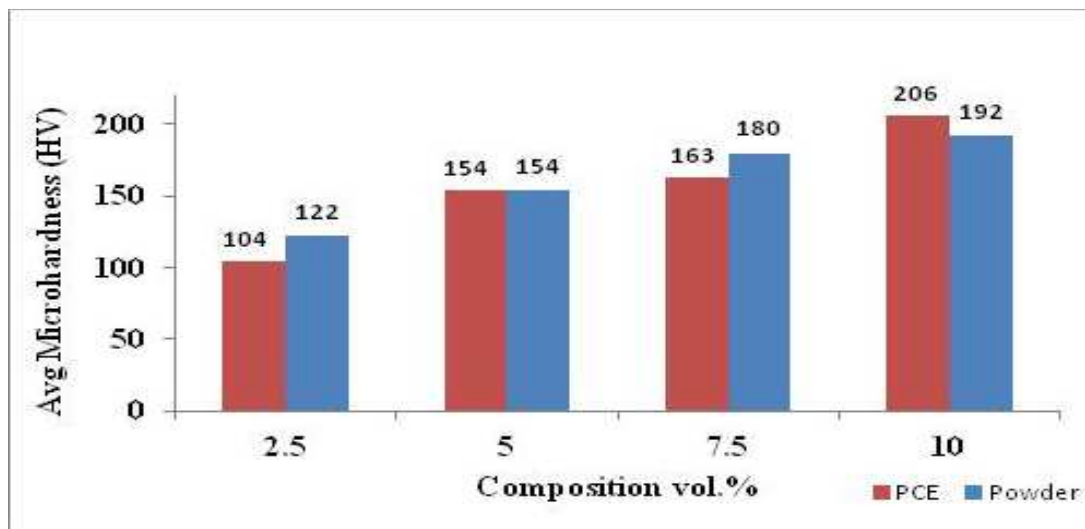


Figure 1: Microhardness for Al-4wt.%Cu-(2.5-10)vol.%SiC nanocomposites bars produced by PCE.

Fig.2 shows the relative density of the Al-4wt.%Cu-(2.5-10) vol. % SiC nanocomposite powder compacts and extruded bars produced as a function of the volume fraction of SiC nanoparticles. The theoretical density of the material components of the composite was used to calculate the relative density of the powder compacts and extruded bars using the rule of mixtures.

From Fig.2, it can be seen that the relative density of the powder compacts decreased

significantly with increasing the SiC nanoparticle contents from 2.5 to 5 vol. % and then changed little with further increase in the SiC nanoparticles to 10 vol. %. This is likely due to the increased hardness of the nanocomposite powder particles, produced by milling, with increasing volume fraction of the hard SiC nanoparticles within the matrix. The relative density of the extruded bars was fairly high, being in the range of 98.5-99.6 %.

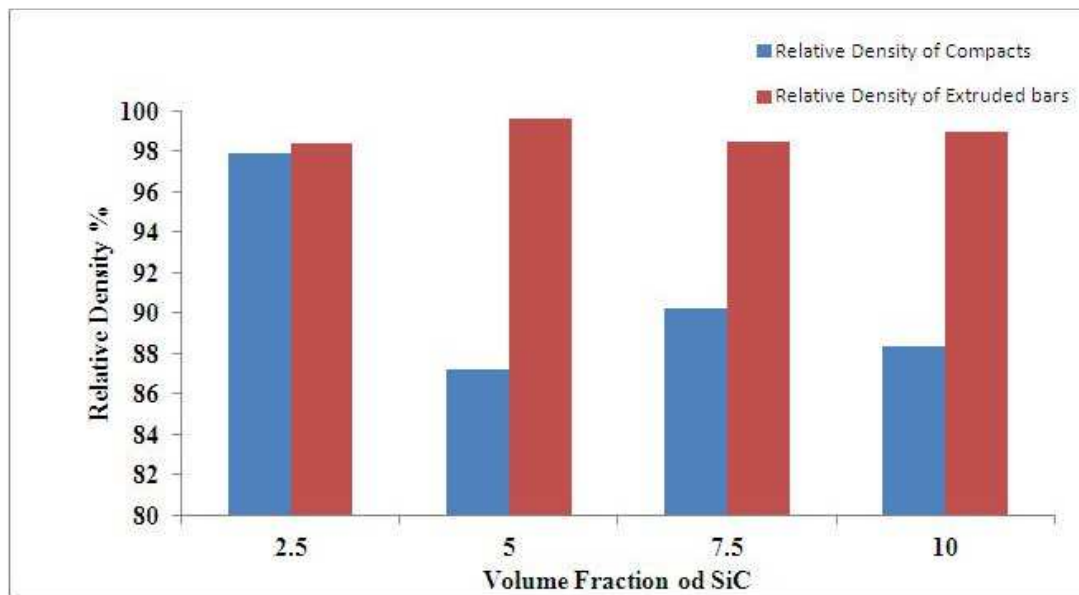


Figure 2: The relative density of the Al-4wt%Cu-(2.5-10_vol.%SiC nanocomposite powder compacts and extruded bars.

During the process of milling mixtures of Al powder with 4wt%Cu and 2.5vol.%SiC nanoparticles together with 1wt%PCA, coarse powder particles with sizes in the range of 20-150 μm formed after 12 hours of milling. When the volume fraction of SiC nanoparticles increased to 5%, the nanocomposite powder particle sizes were in the range of 10-90 μm after 12 hours of milling. When the volume fraction of SiC nanoparticles increased to 7.5%, the nanocomposite powder particle sizes were in the range of 5-120 μm after 12 hours of milling. When the volume fraction of SiC nanoparticles increased to 10%, the nanocomposite powder particle sizes were in the range of 5-70 μm after 12 hours of milling, as can be seen in Figure 3.

Figure 4 shows typical SEM micrographs of the longitudinal sections of the extruded bars. It was clear that the extruded bars were almost fully dense, with the volume fraction of pores less than 1%. The clear discrepancy between the density of the

extruded bars implied by the SEM examination and that measured using the Archimedes' method is caused by an error in the calculation of the theoretical density of the extruded bars using the rule of mixture, since Al and Cu formed a solid solution during milling and consolidation. Fig.5 shows the energy dispersive X-Ray (EDX) elemental mapping of Cu and Si and of the longitudinal sections of the Al-4wt%Cu-(2.5 and 10) vol.%SiC nanocomposite extruded bars. From the elemental mappings of Si and Cu, it was clear that the majority of the SiC nanoparticles and Cu were homogeneously distributed throughout the Al matrix. However, a small volume fraction of the SiC nanoparticles still existed in the Al matrix as agglomerates with sizes in the range of 2-7 μm . Undissolved Cu particles were also occasionally observed in the microstructure of the Al-4wt%Cu-10vol.%SiC extruded bars.

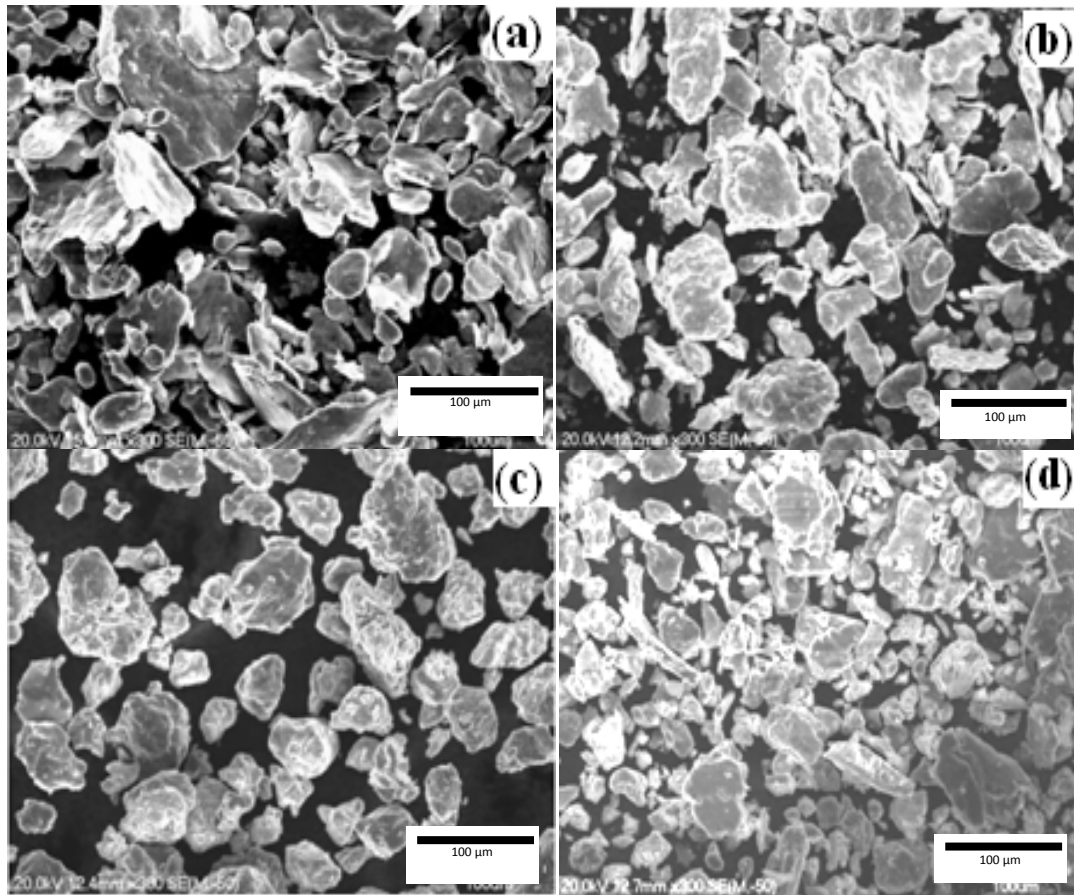


Figure 3: SEM micrographs of Al-4wt%Cu-SiC nanocomposites powder particles produced by 12 hours of milling with 1 wt% PCA: (a) 2.5vol.%SiC, (b) 5vol.%SiC, (c) 7.5vol.%SiC, (d) 10vol. %SiC.

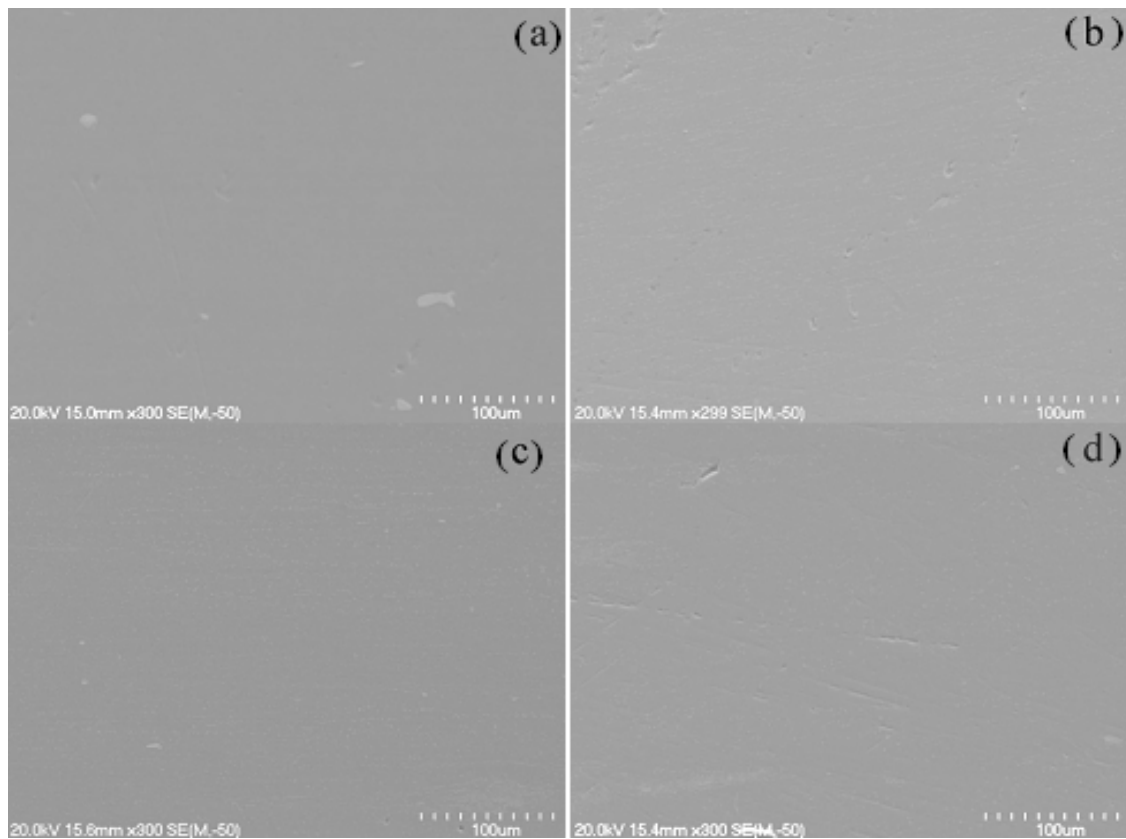


Figure 4: SEM micrographs of the longitudinal cross-sections of the Al-4wt.%Cu-(2.5-10) vol. %SiC nanocomposite bars produced by powder compact extrusion: (a) Al-4wt.%Cu-2.5vol.%SiC ; (b) Al-4wt.%Cu-5vol.%SiC ; (c) Al-4wt.%Cu-7.5vol.%SiC ; and (d) Al-4wt.%Cu-10vol.%SiC.

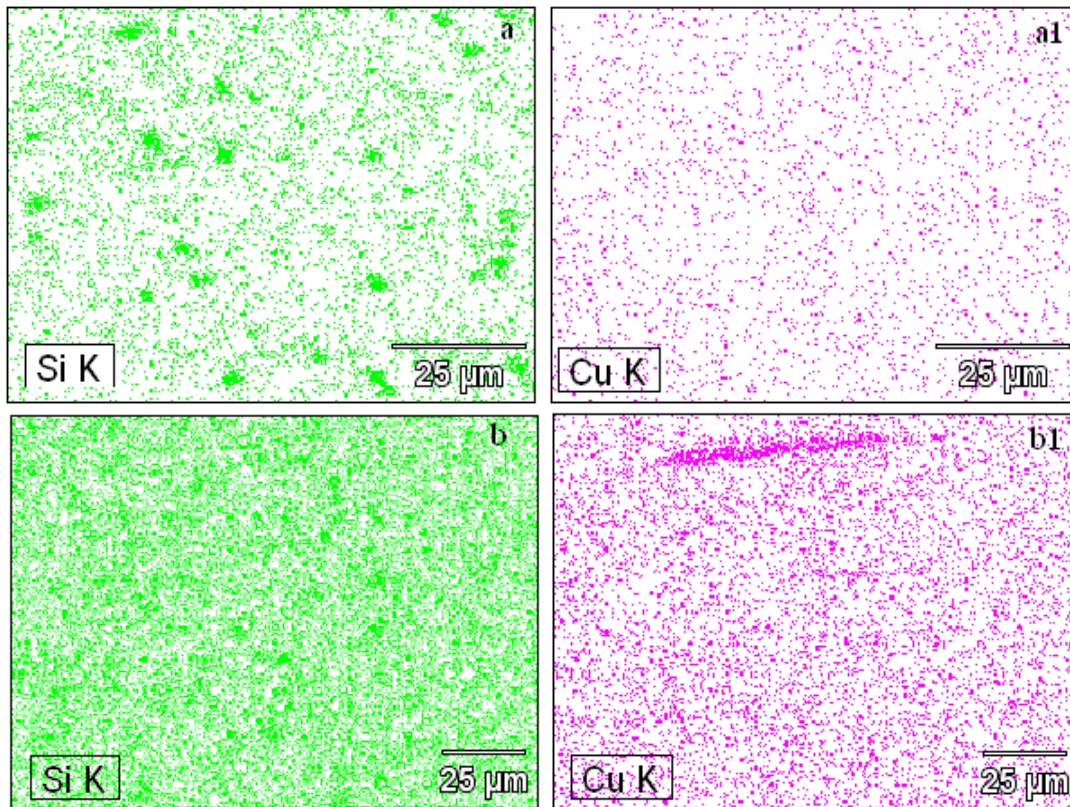


Figure 5: EDX elemental mappings of Si and Cu in the Al-4wt.%Cu-(2.5 and 10) vol. %SiC nanocomposite bars produced by powder compact extrusion: (a) Si distribution in Al-4wt.%Cu-2.5vol.%SiC ; (a1)Cu distribution in Al-4wt.%Cu-2.5vol.%SiC ; (b) Si distribution in Al-4wt%Cu-10vol.%SiC ; and (b1) Cu distribution in Al-4wt%Cu-10vol.%SiC.

Figure 6 shows XRD patterns of Al-4wt%Cu-(2.5-10) vol.%SiC nanocomposite cylindrical bars produced by PCE. The XRD patterns show strong Al peaks with weak SiC and Cu peaks, due to the small sizes and volume fractions of SiC and Cu particles. The average grain sizes and the lattice strain of the Al-4wt%Cu-(2.5-10)vol.%SiC nanocomposites cylindrical bars were estimated based on the broadening of the XRD peaks and using the Williamson-Hall method (Figure 7). Based on the Williamson-Hall method (Figure 7), the estimated average grain size and lattice strain of the Al-4wt%Cu-2.5vol.%SiC nanocomposites were 250 nm and 0.39%, respectively. With increasing volume fraction of SiC nanoparticles to 5 %, the grain size and lattice strain changed to 500 nm and 0.37%, respectively. For Al-4wt%Cu-7.5vol.%SiC nanocomposites, the

grain size and lattice strain were 1250 nm and 0.36%, respectively. For Al-4wt%Cu-10vol.%SiC nanocomposites, the grain size and lattice strain were 1666 nm and 0.42%, respectively. The average grain size increased with increasing volume fraction of the SiC nanoparticles in the nanocomposite, while the lattice strain remained in the same range. This is due to the thermal stability of the microstructure of the Al-4wt%-(2.5-10)vol.% SiC matrix of the nanocomposite which increases with increasing volume fraction of the SiC nanoparticles. This enhances the Zener-drag effect of nanoparticles to resist the movement of grain boundaries. This effect leads to a slower rate of microstructural coarsening with increased content of SiC nanoparticles during powder compact extrusion. Also, the carbide nanoparticles located throughout the composite

microstructure should be obstacles for dislocation movement through the grain and more energy is needed to induce diffusion processes for materials with

higher nanoparticles inclusions. This explains why some crystallite growth were observed at low nano-SiC contents¹⁵.

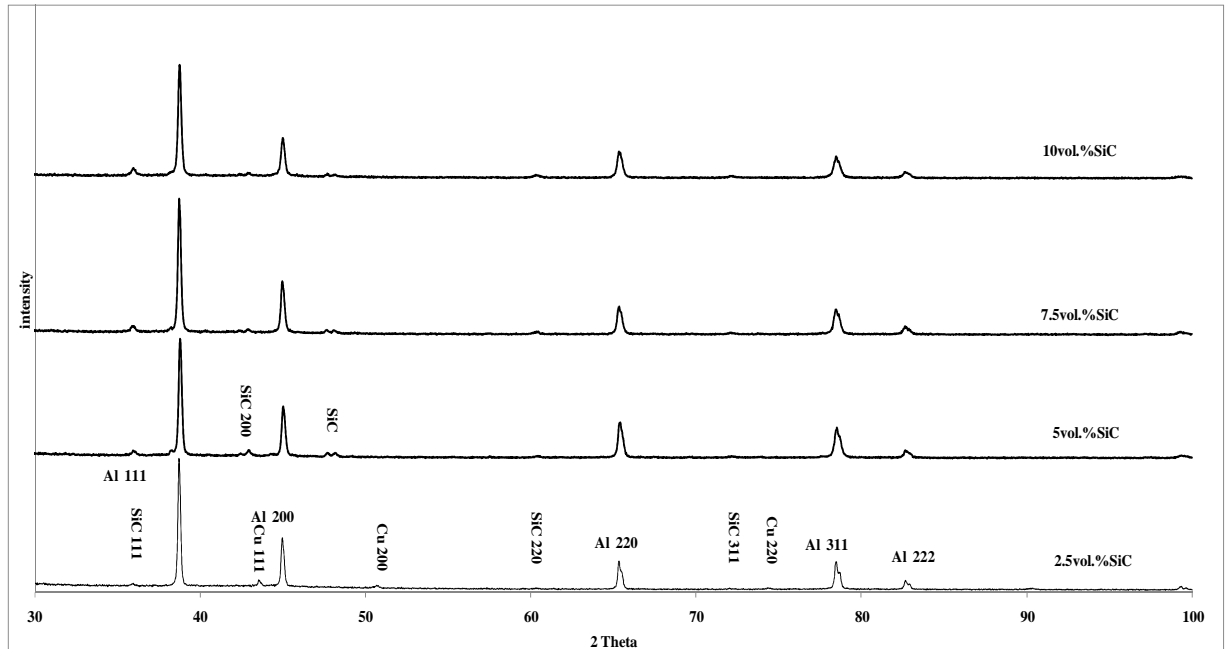


Figure 6: X-ray diffraction patterns of the extruded bars of the Al-4wt.%Cu-(2.5-10) vol.%SiC nanocomposites.

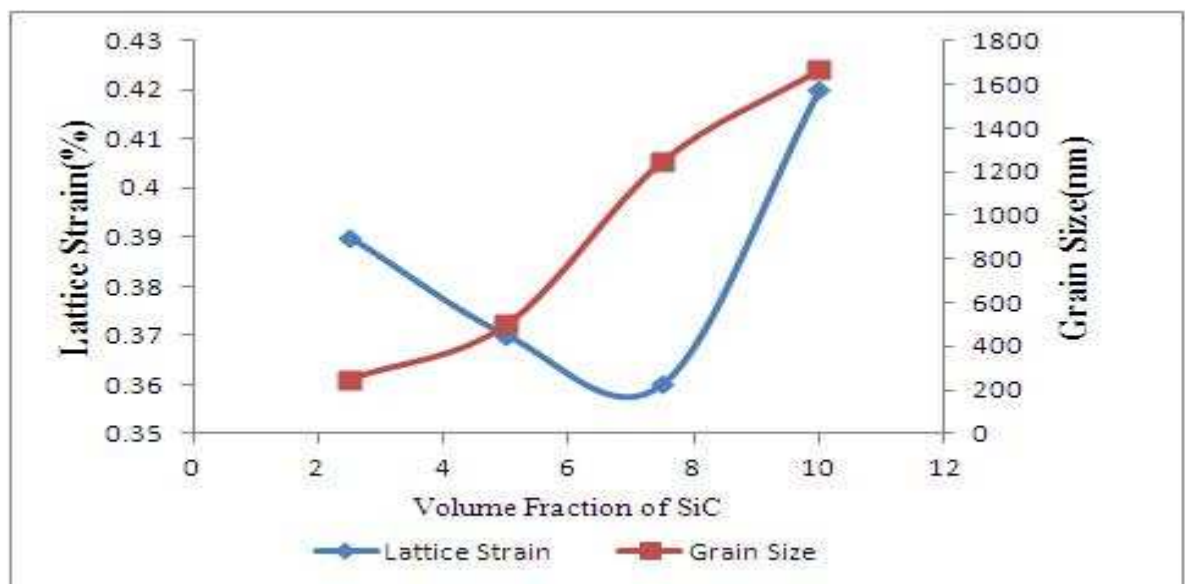
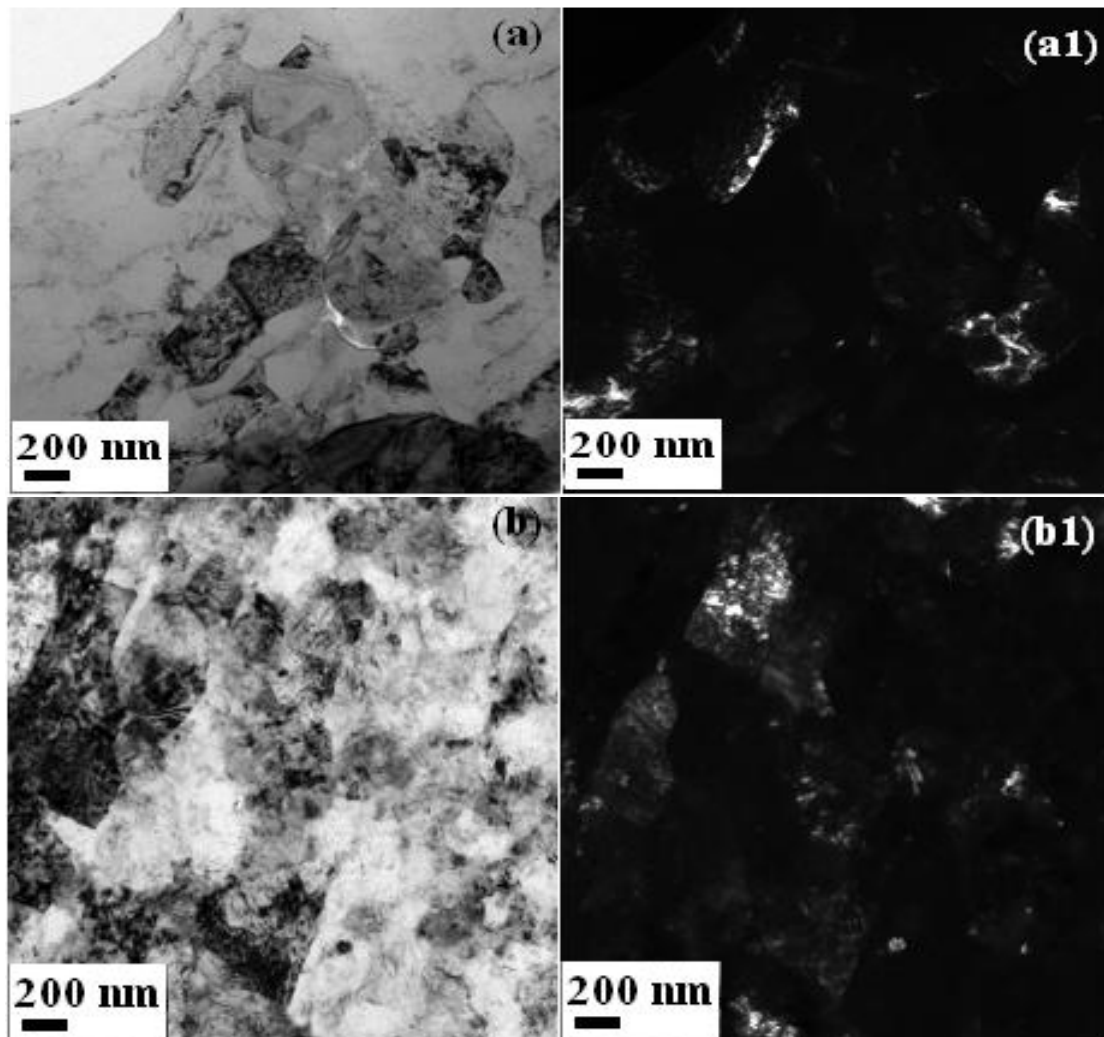


Figure 7: Grain size and lattice strain of the Al-4wt.%Cu-(2.5-10)vol.%SiC nanocomposites bars produced by PCE as a function of the volume fraction of SiC nanoparticles.

TEM was utilised to examine the microstructures of the Al-4wt%Cu-(2.5-10)vol%SiC nanocomposite bars produced by PCE. As shown by the TEM bright field image and dark field images shown in Figure 8, the Al-4wt%Cu-(2.5-10)vol%SiC nanocomposite extruded bars had an ultrafine grained (UFG) microstructure consisting of Al grains with sizes ranging 100-800 nm for Al-4wt%Cu-2.5vol.%SiC, 200-600 nm for Al-4wt%Cu-5vol%SiC, 100-500 nm for Al-4wt%Cu-7.5vol%SiC, and 50-300 nm for Al-4wt%Cu-10vol%SiC. This shows that the average grain size estimated using the broadening of the XRD peaks along with Williamson-Hall method (Figure 7) is clearly bigger than the average Al grain size observed by TEM. This difference is likely due to an underestimate

of the broadness of the XRD peaks. The TEM examination also shows that the Al grains contained a high density of dislocations. Figure 9 shows typical selected area diffraction patterns (SADPs) corresponding to the TEM bright field images shown in Figure 8. The SADPs show diffraction rings of Al {111}, {200}, {220}, and {222} planes, and weak diffraction spots of SiC nanoparticles. This confirms that SiC nanoparticles were incorporated into the microstructure of the Al-4wt%Cu-(2.5-10)vol.% SiC nanocomposite. The contrast showing the SiC nanoparticles was not very clear due to the very small size of SiC nanoparticles and the heavy contrast of the Al matrix grains containing a high density of dislocations.



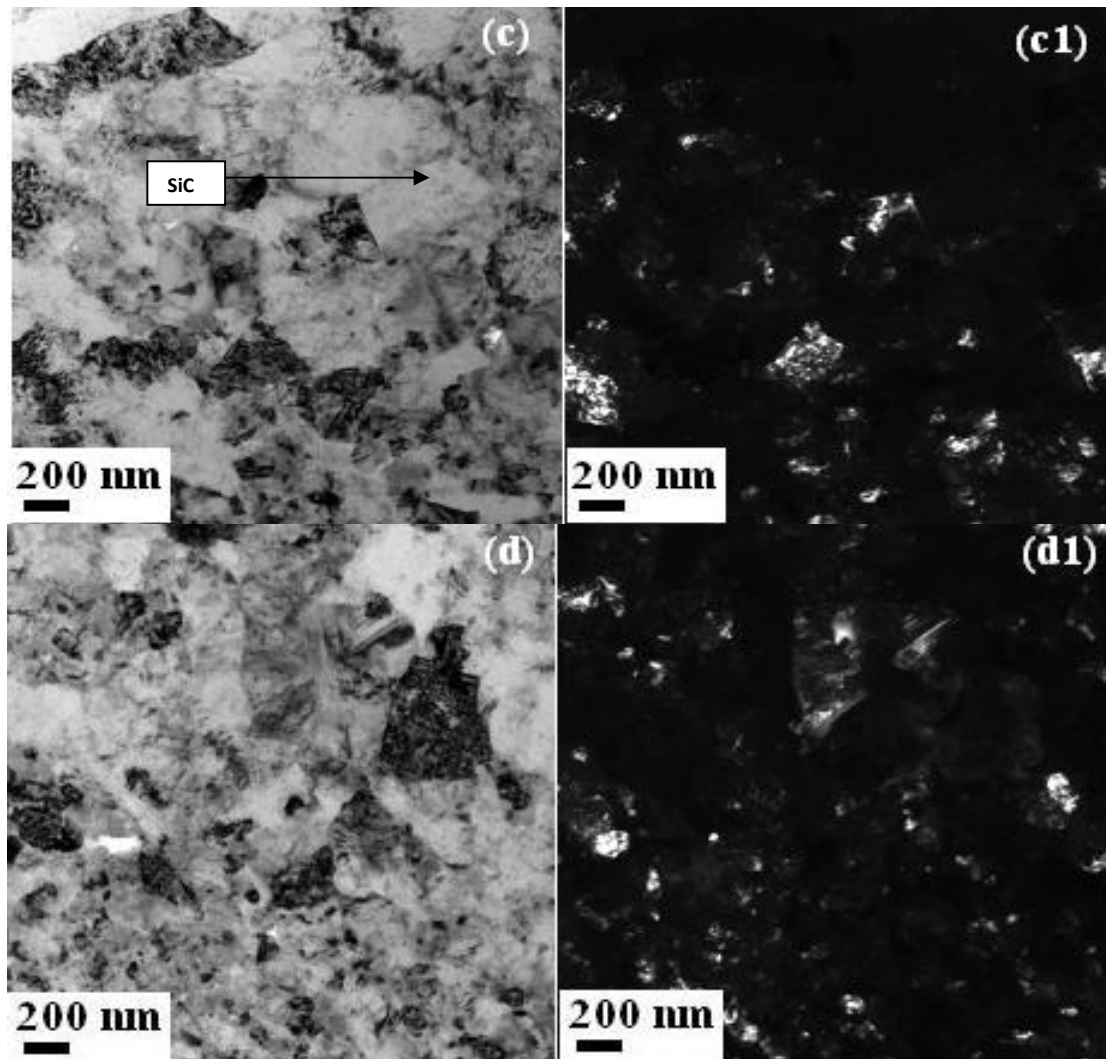


Figure 8 : TEM bright field and dark field images of Al-4wt%Cu-(2.5-10)vol.% SiC nanocomposites bars produced by PCE (a) and (a1) 2.5vol.% SiC,(b) and (b1) 5vol.% SiC,(c) and (c1) 7.5vol.% SiC,(d) and (d1) 10vol.% SiC.

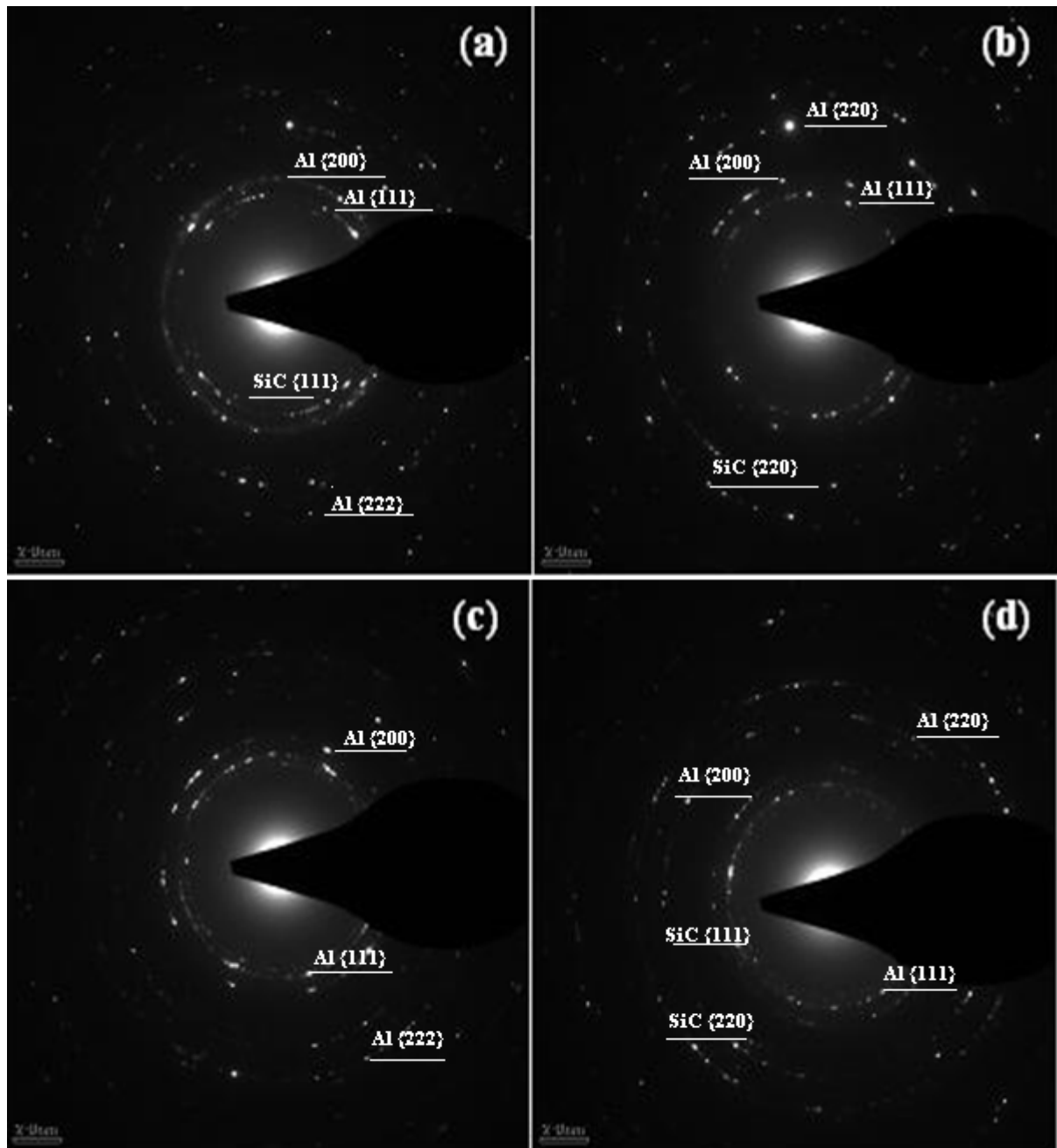


Figure 9: Selected area electron diffraction patterns corresponding to the TEM images in Figure 5.14: (a) Al-4wt%Cu-2.5vol.% SiC, (b) Al-4wt%Cu-5vol.% SiC, (c) Al-4wt%Cu-7.5vol.% SiC, (d) Al-4wt%Cu-10vol.% SiC .

Figure 10 shows the tensile engineering stress-strain curves of specimens cut from the extruded bars. With 2.5 vol. %SiC, the extruded bar showed a yield strength, ultimate tensile strength (UTS) and plastic strain to fracture of 98 MPa, 168MPa and 6.8%, respectively. By increasing the volume fraction of SiC nanoparticles to 5%

the yield strength and UTS of the extruded bar increased dramatically 391MPa and 400MPa, respectively, but the plastic strain to fracture of the extruded bar decreased to 1.2%. With a further increase in the volume fraction of SiC nanoparticles to 7.5 or 10 vol.%, the tensile test specimens fractured prematurely at stresses of 270 MPa and

325 MPa respectively, without showing any plastic yielding. Figure 11 shows the typical fracture surfaces of the tensile test specimens cut from the Al-4wt%Cu-(2.5-10) vol. %SiC bars produced by PCE. It can be seen that the fracture of the Al-4wt%Cu-(2.5 and 5) vol. % SiC nanocomposite specimens occurred through ductile fracture of the Al matrix, with the fracture surfaces showing dimples and ligaments. It appeared that with increasing the SiC nanoparticle content from 2.5 vol. % to 5%, the depth of the dimples and height of the ligaments became significantly smaller, as shown in Figure 11 (a) and (b). The fracture surfaces of the Al-4wt%Cu-(7.5 and 10) vol. %SiC nanocomposite

specimens were very flat, suggesting that their fracture was brittle in nature. To reveal more information about the nature of the bonding between the powder particles, the longitudinal sections of the fractured specimens just below the fracture surfaces were also examined using SEM, as shown in Figure 12. It can be seen that only a few cavities (indicated by the arrows) formed near the fracture surfaces during tensile deformation and fracture of the specimens. The shapes of the cavities suggest that they were not caused by separation of neighbouring powder particles due to weak interparticle bonding in the broken tensile test specimens.

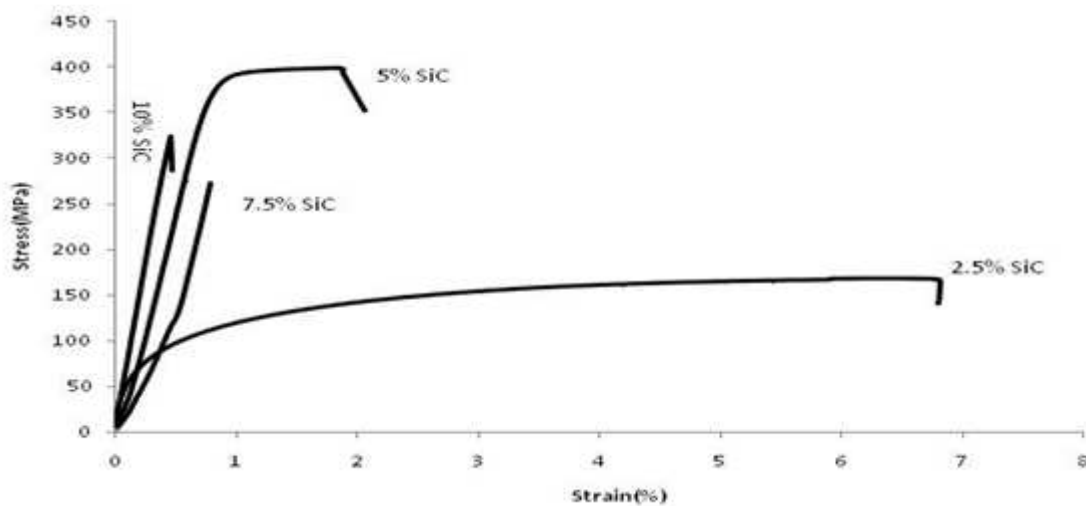


Figure 10 : Tensile stress-strain curves of specimens cut from Al-4wt%Cu-(2.5-10) vol. % SiC bars produced by PCE.

This work has shown that with increasing the volume fraction of SiC nanoparticles, the microstructure of the Al-4wt%Cu matrix of the bulk nanocomposite samples becomes fine. There are two reasons for this. The first reason is that an increase in the content of SiC nanoparticle content in the starting powder microstructure increases the effectiveness of HEMM, causing the microstructure of the nanocomposite powder produced by HEMM to be finer, as confirmed by TEM examination of the milled powder particles¹⁶. The second reason is that the thermal stability of the microstructure of the Al-4wt%Cu matrix of the nanocomposites increases with the

increasing volume fraction of SiC nanoparticles due to the increased Zener-drag effect of nanoparticles to resist the movement of grain boundaries. This effect leads to slower rate of microstructural coarsening with increased content of SiC nanoparticles.

As expected, the yield strength of the bulk nanocomposite samples increases significantly from 98 to 391 MPa with increasing volume fraction of the SiC from 2.5 to 5 vol. %, showing that SiC nanoparticles are effective in strengthening the materials. In the meantime, the further refinement of the microstructure of the Al-4wt%Cu matrix can also contribute to the

increase of the yield strength. The high effectiveness of these two factors in strengthening the composite is also reflected by the observation that the yield strength of the ultrafine structured Al-4wt%Cu-5vol.%SiC nanocomposite (391 MPa) is more than 2.5 times higher than that of the coarse structured Al-4wt%Cu-10vol.%SiC composite with an average particle size of $23\mu\text{m}$ ¹⁷. The significant decrease in ductility of the bulk nanocomposite samples with the increasing volume fraction of SiC nanoparticles, from 2.5 to 5%, may be due to two reasons: the existence of SiC nanoparticle agglomerates in the microstructure, which makes the formation of cavities under tensile stress easier, and

the refinement of microstructure of the Al-4wt%Cu matrix which makes it easier to lose stability of deformation under tension¹⁸. Similarly, the premature fracture of the Al-4wt%Cu-(7.5 and 10)vol.%SiC nanocomposite samples during tensile testing may also be due to the existence of SiC nanoparticle agglomerates in their microstructure, which make it very easy to form cavities under tensile stress. With the total volume fraction of the SiC nanoparticles being at a high level of 7.5 or 10%, the number of such SiC nanoparticles agglomerates per unit volume of the sample can be quite high, so it is easy for cracks to form and propagate, causing fracture to occur before macroscopic yielding.

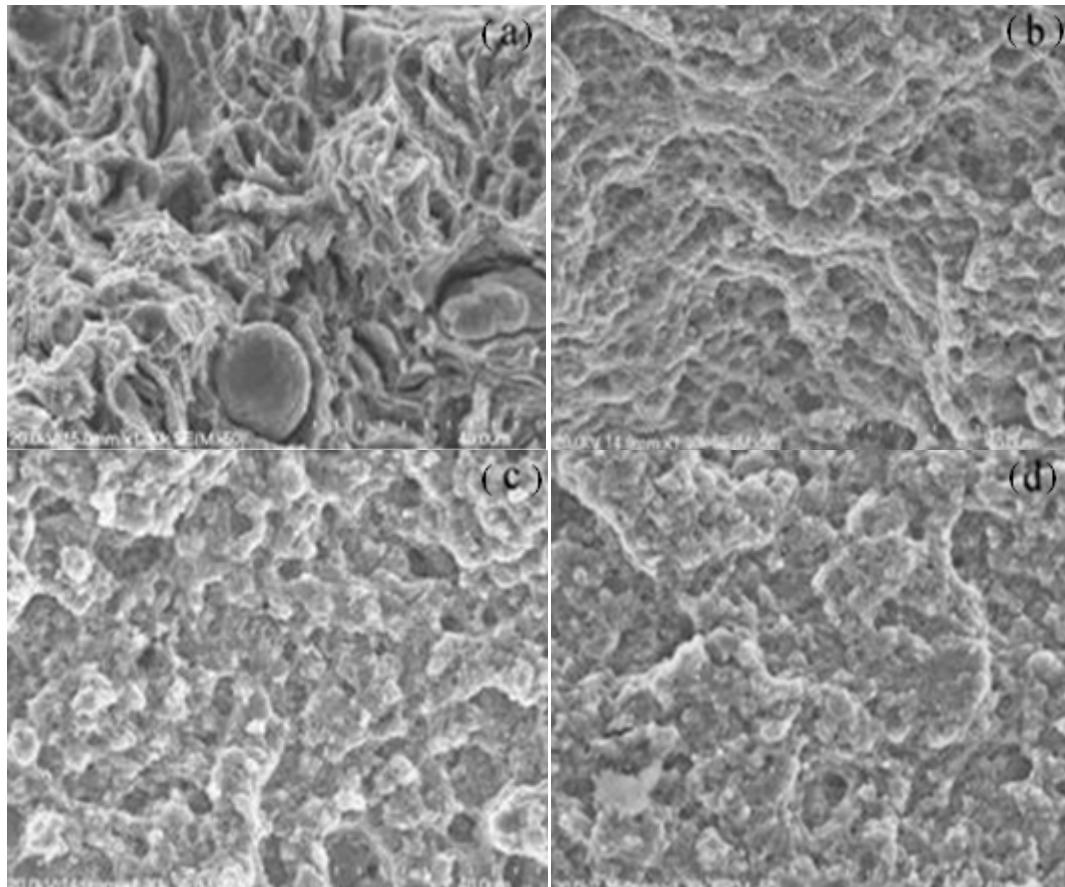


Figure 11: SEM micrographs of the fracture surfaces of the tensile test specimens cut from Al-4wt%Cu-(2.5-10) vol.% SiC nanocomposite bars produced PCE: (a) 2.5vol. %SiC (b) 5 vol. %SiC (c) 7.5vol. %SiC (d) 10vol. %SiC.

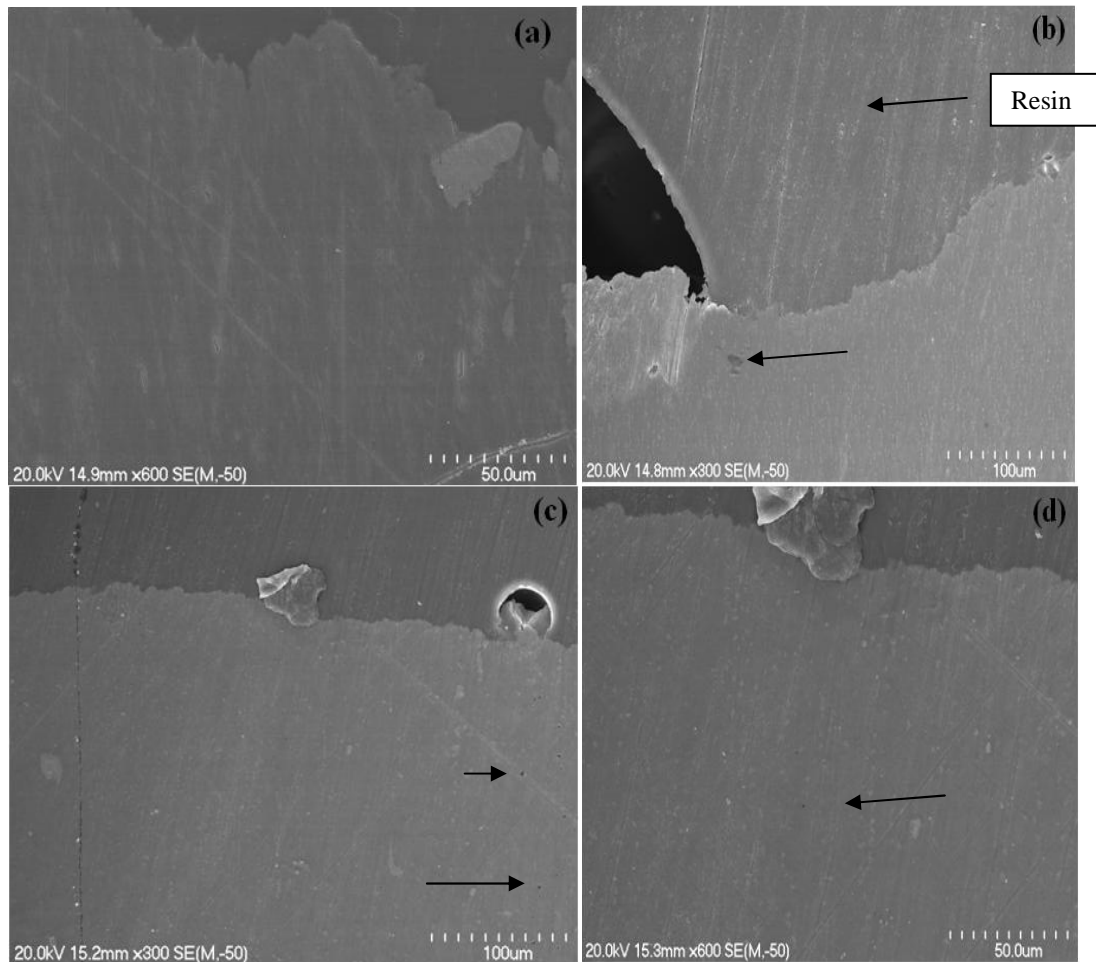


Figure 12: SEM micrographs of the longitudinal sections just below the fracture surfaces of the tensile test specimens cut from the Al-4wt%Cu-(2.5-10)vol.% SiC nanocomposite bars produced by PCE: (a) 2.5vol.% SiC ; (b) 5vol.% SiC ; (c) 7.5vol.% SiC; (d) 10vol.% SiC.

Conclusion

Ultrafine structured Al-4wt.%Cu-(2.5-10) vol. % SiC nanocomposite bars have been produced by a combination of high energy ball milling (HEMM) of mixtures of Al and Cu powders and SiC nanopowder followed by consolidation of the milled powder. Increasing the volume fraction of SiC nanoparticles from 2.5 to 5 % causes the yield strength, ultimate tensile strength and microhardness of the nanocomposites to increase from 98 MPa, 168 MPa and 104 HV to 391 MPa, 400 MPa and 205 HV, showing the high effectiveness of SiC nanoparticles and microstructure refinement in strengthening the material. However, the ductility decreases from 6.8% to 2 %, possibly due to the existence of SiC nanoparticle agglomerates in the Al-

4wt%Cu-5vol.%SiC nanocomposite. The ultrafine structured Al-4wt%Cu-(7.5 and 10)vol.%SiC nanocomposite bars fractured prematurely during tensile testing. The possible reason for this may be the existence of SiC nanoparticles agglomerates in their microstructure

References

1. Monazzah A.H, Simchi A. and Reihani S.M.S.(2010) " Creep behaviour of hot extruded Al-Al₂O₃ nanocomposite powder," Material Science and Engineering A, 527, 2567-2571.
2. Huang Y.G, Chen Z.G and Zheng Z.Q. (2011) "A conventional thermo-mechanical process of Al-Cu-Mg alloy for increasing

ductility while maintaining high strength,” *Scripta Materialia*, 64,382-385.

3. Ahamed H. and Senthilkumar V. (2010) “Role of nano-size reinforcement and milling on the synthesis of nano-crystalline aluminium alloy composites by mechanical alloying,” *Journal of Alloys and Compounds*, 505,772-782.

4. Alizadeh M. and Paydar M.H. (2010) “Fabrication of nanostructure Al/SiC_p composite by accumulative roll-bonding(ARB) process,” *Journal of Alloys and Compounds*,492 ,231-235.

5. Wang Z., Song M., Sun C., and Y. He. (2011) “Effect of particle size and distribution on the mechanical properties of SiC reinforced Al-Cu alloy composite,” *Material Science and Engineering A*, 528, 1131-1137.

6. Kollo L., Leparoux M., Bradbury C.R., Jaggi C., Carreno-Morelli E., and Rodriguez-Arbaizar M. (2010) “Investigation of planetary milling for nano-silicon carbide reinforced aluminium metal matrix composite,” *Journal of Alloys and Compounds*, 489, 394-400.

7. Gazawi A., Zhang D.L., Pickering K.L. , and Mukhtar A. (2011) “Microstructure and Mechanical Behaviour of Ultrafine Grained Al-4wt%Cu-(2.5-10) vol.% SiC Metal Matrix Composites Produced by Powder Compact Forging,” *Advanced Materials Research*, 275, 208-213.

8. Kamrani S., Riedel R., Reihani S.M.S., and Kleebe H.J. (08/2007) “Effect of Reinforcement Volume Fraction on the Mechanical Properties of Al-SiC Nanocomposites Produced by Mechanical Alloying and Consolidation,” *Powder Metallurgy*, 50(3), 276-282.

9. Goussous S., Xu W. and Xia K. (2010) “Developing aluminium nanocomposites via severe plastic deformation,” *Journal of Physics Conference*, 240.

10. Rahimian M., Ehsani N., Parven N., and Baharvandi H.R. (2009) “The effect of particle size, sintering temperature and sintering time on the properties of Al-

Al₂O₃ composites , made by powder metallurgy,” *Journal of Materials Processing and Technology*, 209, 5387-5393.

11. Hesabi Z.R., Simchi A., Reihani S.M.S , and Simancik F. (2010) “Fabrication and characterization of ultrafine-grained Al-5vol.%Al₂O₃ nanocomposite,” *International Journal of Nanomanufacturing*,” 5, 341-351.

12. Narayanasamy R., Ramesh T., and Prabhakar M.(2009) “Effect of particle size of SiC in aluminium matrix on workability and strain hardening behaviour of P/M composite,” *Materials Science and Engineering A*, 504,13-23.

13. Ogel B. and Gurbuz R. (2001) “Microstructural characterization and tensile properties of hot pressed Al-SiC composites prepared from pure Al and Cu powders,” *Materials Science and Engineering A*, 301, 213-220.

14. Kollo L., Leparoux M., Bradbury C.R., Veinthal R., Jaggi C., Carreno-Morelli E., Rodrigues-Arbaizar M. (2010) “Investigation of planetary milling for nano-silicon carbide reinforced aluminium metal matrix composites,” *Journal of Alloys and Compounds*, 489, 394-400.

15. Kollo L., Bradbury C.R., Veinthal R., Jaggi C., Carreno-Morelli E., Leparoux M. (2011) “Nano-silicon carbide reinforced aluminium produced by high energy milling and hot consolidation,” *Materials Science and Engineering A*, 528, 6606-6615.

16. Amro A. Gazawi, Deliang Zhang, Charlie Kong, Paul Munroe, unpublished research.

17. Gupta M.,Lai M.O. and Soo C.Y. (1996) “Effect of type of processing on the microstructural features and mechanical properties of Al-Cu/SiC metal matrix composites,” *Materials Science and Engineering A*, 210, 114-122.

18. Departement of Materials science and Engineering, John Hopkins University.(2003) “Nanocrystalline materials: controlling plastic instability.” *Nature Materials*, 2(1), 7-8.